Supporting information

Single-molecule Scale Quantification Reveals Interactions Underlying Protein-protein Interface: From Forces to Non-covalent Bonds

Heng Sun, Yichen Tian, Yuna Fu, Yongrong Lei, Yani Wang, Xinrui Yan, Xinyu Kuang, Jianhua Wang*

Dynamic force spectroscopy model to quantitatively analyze the interaction of BAX/Bcl-2 interface

the Bell-Evans (BE) model [1, 2]

$$F = \frac{k_B T}{x_\beta} \times \ln\left(\frac{r\chi_\beta}{k_{off}^0 k_B T}\right) \quad (1)$$

$$\frac{1}{\tau(F)} = k_{off}^0 \exp\left(\frac{F\gamma}{k_B T}\right) \quad (2)$$

where k_B is the Boltzmann constant, T is the absolute temperature, χ_β is the distance between bound and transition state, k_{off}^0 is dissociation rate, r is loading rates, *F* is the external force. τ is the bond lifetime, which is giving by Equation 2 using the k_{off}^0 and x_β taken from Eq. 1. Generally, a higher association rate to the protein binding pocket and a longer bond lifetime indicates that the complex is stable, Fig. S3B. The height energy barrier (ΔG_β) can be estimated by putting the k_{off}^0 into Eq. (3):

$$\Delta G_\beta = - k_B T \ln \frac{k_{off}^0 h}{k_B T} \quad (3)$$

where h is the Planck's constant.

The Dudko–Hummer–Szabo (DHS) model [3, 4]

$$F = \frac{\Delta G_\beta}{\nu x_\beta}\left\{1 - \left[\frac{k_B T}{\Delta G_\beta}\ln\frac{k_{off}^{0} k_B \mathrm{T}\exp\left(\frac{\Delta G_\beta}{k_B T}\right)}{x_\beta r_F}\right]^{\nu}\right\} \quad (4)$$

In this model, ν represents the free-energy profile, giving the linear cubic model (ν = 2/3), the cusp model (ν = 1/2), compared to the Bell–Evans formula (ν = 1). $^{\Delta G_\beta}$ is the height energy barrier. The bond lifetime is approximated by:

$$\tau(F) \cong \frac{[\frac{\pi}{2}(\langle F^2\rangle - \langle F\rangle^2)]^{1/2}}{r(F)} \quad (5)$$

where $\langle F^2\rangle$ is the mean squared rupture force at a given loading rate *r*(*F*), Fig. S3C.

the Frididdle-Noy-De Yoreo (FNDY) model [5]

The process of bonds rupture goes through two phases: an equilibrium phase at lower LR, where the bonds break and rebinds, and a kinetic phase at higher LRs, where the bonds break irreversibly. The transition between the two phases occurs at equilibrium forces ($^{F_{eq}}$) and is described with Eq. 6:

$$F_{eq} = \sqrt{2k_{eff}\Delta G_{bu}} \quad (6)$$

where $^{F_{eq}}$ is equilibrium force, $^{k_{eff}}$ is the effective spring constant of the entire system (see Fig. 2H from main text); $^{\Delta G_{bu}}$ is equilibrium free energy and represents the energy difference between the unbound and bound states. The unbinding force and dissociation rate are defined by the Eq. 7 and 8:

$$F \cong F_{eq} + f_\beta \ln\left(1 + e^{-\gamma}\frac{r}{k_{off}(F_{eq}) f_\beta}\right) \quad (7)$$

$$k_{off} = \frac{k_{off}(F_{eq})}{\exp\left[\frac{1}{k_B T}\left(F_{eq} x_\beta - \frac{k_{eff} {x_\beta}^2}{2}\right)\right]} \quad (8)$$

where $f_\beta = \frac{k_B T}{x_\beta}$ is the thermal scaling factor and γ = 0.577 is Euler's constant.

Estimation of association rate for BAX/Bcl-2

A relationship between the interaction time and BP is described with Eq. 9 [6, 7]:

$$BP = A * \left[1 - \exp\left(\frac{-(t - t_0)}{\tau}\right)\right] \quad (9)$$

where A is the maximal BP and t_0 is the lag time, τ is the time required for the half-maximal binding probability. By assuming the BAX/Bcl-2 follows pseudo-first-order dynamics, the value of k_{on} is estimated by applying the expression:

$$k_{on} = \frac{V_{eff} \cdot N_A}{n_b \tau} \quad (10)$$

where V_{eff} is the effective volume of a sphere describing the protein binding pair, N_A is Avogadro's number, and n_b is the number of binding partners.

Poisson Statistical Method

We calculated the strength of the single bond between the BAX/Bcl-2 interfaces using Poisson statistics, which is similar to the approach we previously used in the single molecule force analysis [8, 9]. At the maximum unbinding force distribution, the distribution of the number of multiple interacting pairs follows a Poisson distribution, expressed as:

$$P(N) = \frac{e^{-\lambda}\lambda^N}{N!} \quad (11)$$

$$\sigma_n^2 = \lambda \quad (12)$$

where $P(N)$ is the probability of forming N number of binding bonds, λ and σ_n^2 represent the mean and variance of the multiple bonds formed in the unbinding events, respectively. Then the unbinding force values for each set of measurements will follow the following equation:

$$F_{av} = \lambda F_i + F_0 \quad (13)$$

$$\sigma_F^2 = (\sigma_n F_i)^2 = \lambda F_i^2 \quad (14)$$

where F_i is the single bond specific force, F_0 is the non-specific force, F_{av} is the mean value of unbinding force and σ_F^2 is the variance of unbinding force. Therefore, we obtain the following expression:

$$\sigma_F^2 = \lambda F_i^2 = F_{av}F_i - F_iF_0 \quad (15)$$

The measurements were performed at several randomly selected points corresponding to different substrate locations, each providing 50-60 individual force measurements (Table S2). The mean and variance were then calculated from the measured forces, a curve of variance versus mean was plotted, and F_i and F_0 can be derived from the linear regression (see Fig. 5A from main text).

Characterization of surface energy and surface parameters of the BAX/Bcl-2 interface

By performing contact angle analysis on the surface using three different probe liquids (water, ethylene glycol, and diiodomethane) with known surface tension (γ), the values of the surface energy components were determined by combining the three equations [10-14]:

$$0.5(1 + cos\theta)\gamma_L = \sqrt{\gamma_S^{LW}\gamma_L^{LW}} + \sqrt{\gamma_S^+\gamma_L^-} + \sqrt{\gamma_S^-\gamma_L^+} \quad (16)$$

where θ is the contact angle formed between a droplet of liquid (L) and the surface of component (S), γ is the surface tension, LW is the component of Lifshitz–van der Waals，+ and – are electron acceptor and electron donor component, respectively. The values of surface tension of the three test liquids are displayed in Table S3.

According to the theory of Van Oss [10, 12, 15, 16], the interfacial free energy of interaction between two molecules in water is expressed as:

$$\Delta G_{i(W)i} = 2(\sqrt{\gamma_1^{LW}\gamma_w^{LW}} + \sqrt{\gamma_2^{LW}\gamma_w^{LW}} - \sqrt{\gamma_1^{LW}\gamma_2^{LW}} - \gamma_w^{LW} + \sqrt{\gamma_w^+}\left(\sqrt{\gamma_1^-} + \sqrt{\gamma_2^-} - \sqrt{\gamma_w^-}\right) + \sqrt{\gamma_w^-}\left(\sqrt{\gamma_1^+} - \sqrt{\gamma_1^+\gamma_2^-} - \sqrt{\gamma_2^+\gamma_1^-}\right)) \quad (17)$$

where γ_1 and γ_2 are surface energy of BAX and Bcl-2 molecule, respectively. γ_w is the surface energy of water.

Supplementary Figures

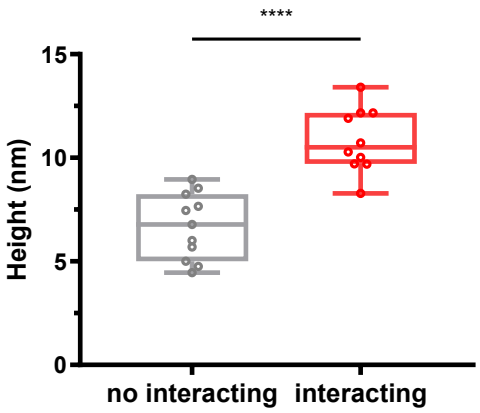

Figure S1. Comparison between height of the BAX interacting with BAX versus the not interacting. The height values were extracted from the topography of Bcl-2 probed with BAX-functionalized tips with contact mode. The BAX/Bcl-2 interacting possess a significantly higher height compared to the not interacting. The min/ max of the box the 25th and 75th percentiles respectively, and the whiskers the s.d. of the mean value. The line in the box indicates the median. **** indicates p-values <0.0001 on unpaired sample t tests.

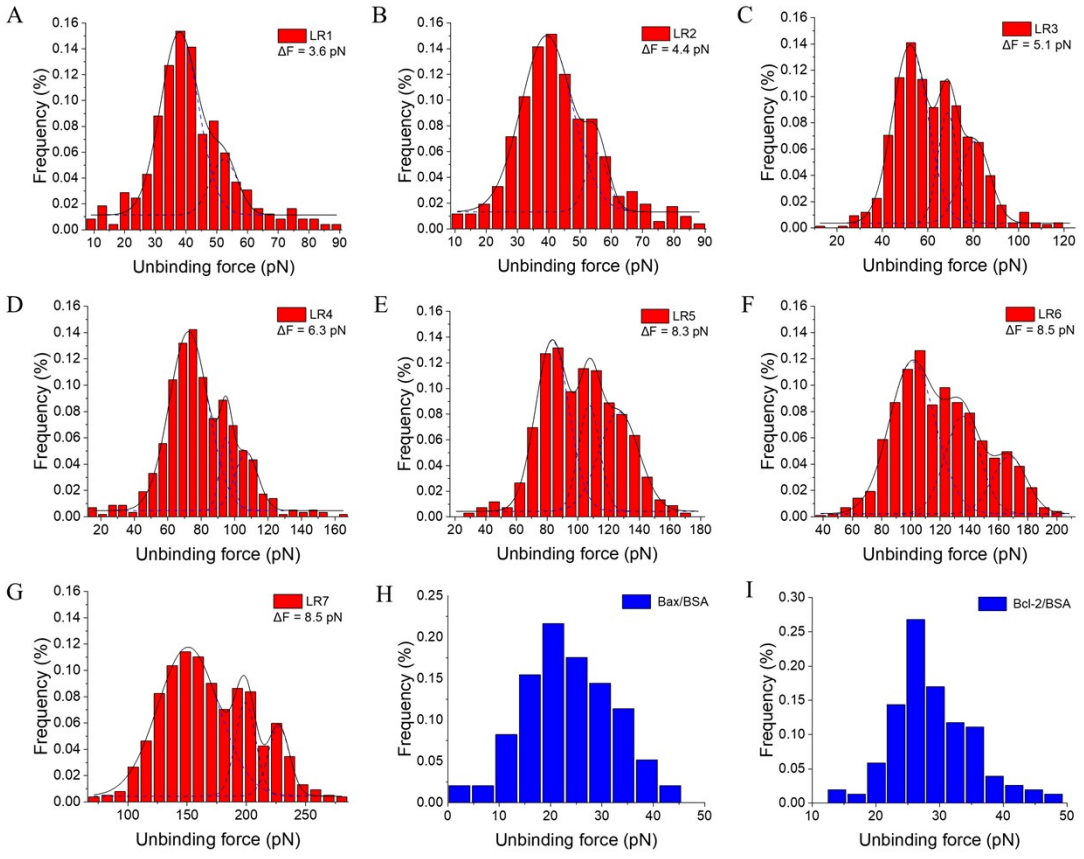

Figure S2. Unbinding forces frequency distributions of binding events. (A-G) frequency distributions of unbinding forces in LR ranges #1-7 for BAX/Bcl-2 interactions. Multi-peak Gaussian fits are used to extract the most probable unbinding force for each LR range. (H-I) Frequency distribution of unbinding force for non-specific binding events at a loading rate of 1 μm/s. (H) BAX/BSA. (I) Bcl-2/BSA.

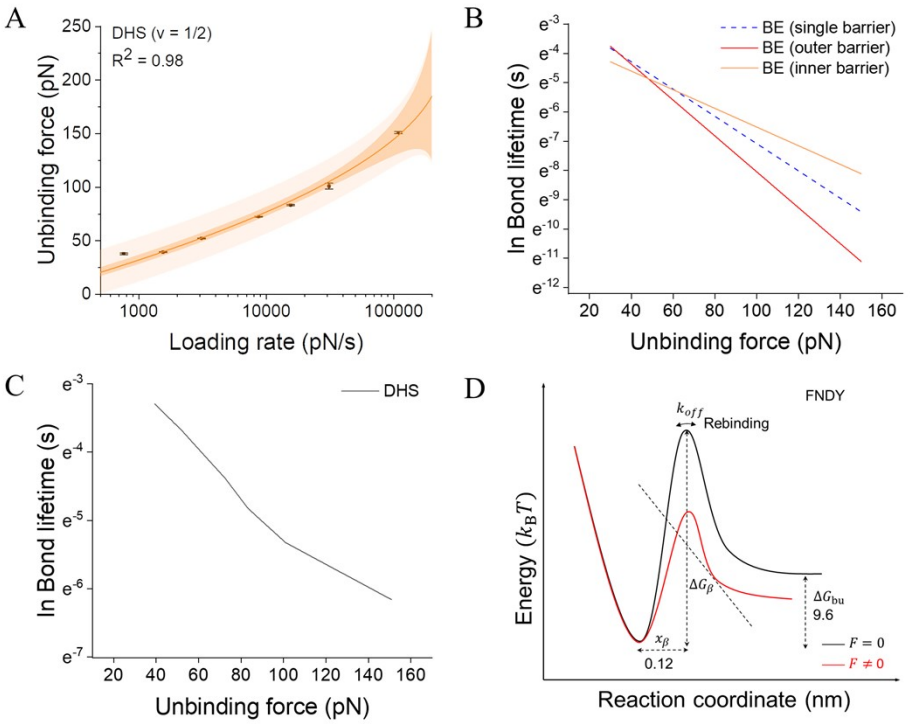

Figure S3. (A) Force spectra are fitted with the DHS model, ν = 1/2. (B and C) The relationship between bond lifetime and unbinding force for Bell-Evans (B) and DHS (C) model. (D) Conceptual cartoons of the binding energy landscape of single BAX/Bcl-2 bonds, describing one barrier with possible rebinding.

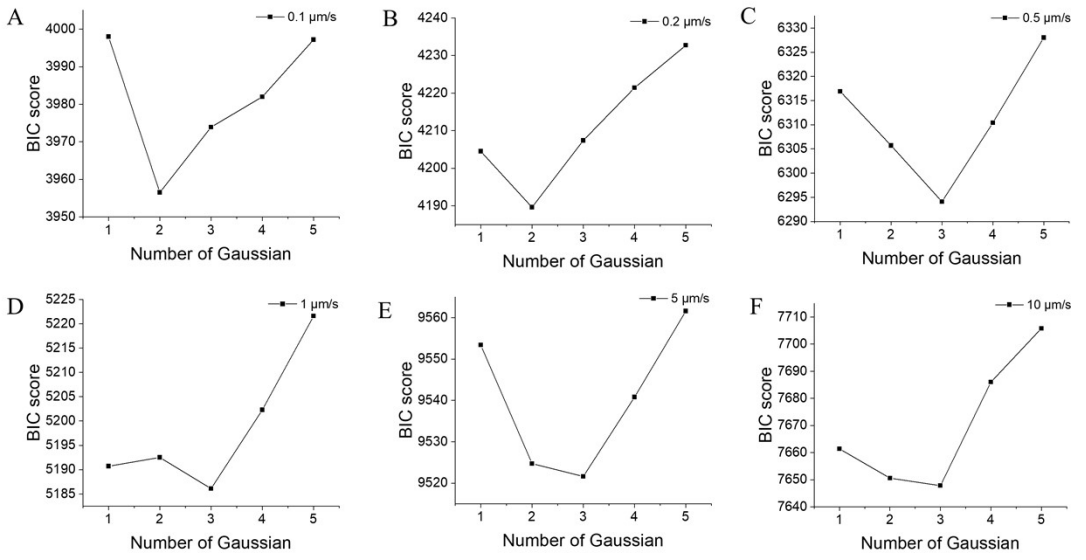

Figure S4. (A-F) Bayesian information criterion (BIC) predicts the optimal number of Gaussians in the unbinding forces histograms in Fig. S2.

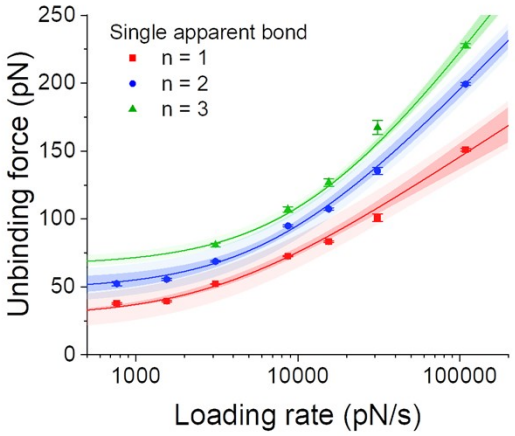

Figure S5. Most probable unbinding forces as a function of LR are plotted on a logarithmic scale. Force spectra data are fitted with single apparent bonds FNDY model. F_{eq}, x_{β}, and $k_{off}(F_{eq})$ are set as free parameters fits for each set of independent single bonds. The error bars represent the Gaussian-fit SD of the corresponding histogram. Darker shaded areas represent 95% confidence intervals, and lighter shaded areas represent 95% of prediction intervals of the fit.

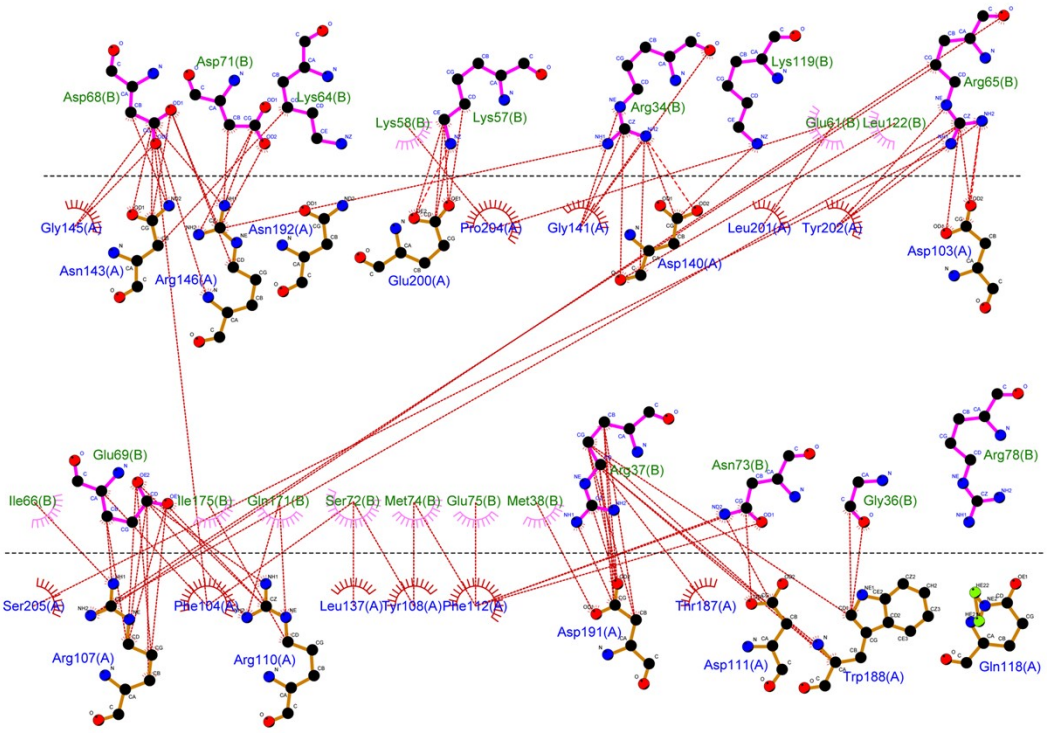

Figure S6 Residues of BAX involved in the hydrophobic interaction network are indicated in green, whereas Bcl-2 is indicated in blue. The hydrophobic network diagram is generated using LIGPLOT.

Supplementary Tables

Table S1 Kinetic and energy landscape paraments obtained with FNDY models for multiple bonds between BAX and Bcl-2 proteins, where each set of data was fitted individually under the assumption of single apparent bonds acting.

No. of bonds	F_{eq} (pN)	f_{β} (pN)	$k_{off}(F_{eq})$ (S^{-1})	k_{off} (S^{-1})	x_{β} (nm)	τ (S)	ΔG_{bu} (k_BT)
n = 1	28.02 ± 0.54	34.25 ± 1.32	54.31 ± 4.24	24.38 ± 0.07	0.12 ± 0.01	0.041	9.6 ± 1.11
n = 2	48.18 ± 3.84	58.71 ± 6.87	75.29 ± 13.29	33.74 ± 0.04	0.07 ± 0.01	0.030	26.57 ± 4.48
n = 3	66.02 ± 3.93	82.2 ± 3.57	96.29 ± 11.36	43.52 ± 1.25	0.05 ± 0.004	0.023	42.35 ± 5.64

n = 1[a]	34.25 ± 1.32		24.38 ± 0.07	0.12 ± 0.01		0.041
n = 2 [a]	58.71 ± 6.87		15.67 ± 0.69	0.14 ± 0.02		0.064
n = 3 [a]	82.2 ± 3.57		9.39 ± 0.61	0.15 ± 0.01		0.106

[a] the transition state distance (x_β) is corrected using n, $f_\beta^{app} = \left(\frac{k_B T}{\frac{x_\beta}{n}}\right)$.

Table S2. Unbinding forces between BAX/Bcl-2 pairs at a loading rate of 1 µm/s. Error propagation is used to determine the uncertainty of the calculated values.

Mean force (λ)	Variance of force (σ_F^2)	Number of sets	Mean number bonds (n)
67.42 ± 5.1	26.64	48	2.77 ± 0.23
73.32 ± 11.3	130.26	52	3.01 ± 0.48
76.08 ± 14.7	219.35	53	3.13 ± 0.62
77.27 ± 14.0	199.88	52	3.18 ± 0.59
79.18 ± 16.3	269.38	51	3.26 ± 0.68
82.53 ± 18.1	333.95	58	3.40 ± 0.75
86.45 ± 20.9	449.07	51	3.56 ± 0.87
92.30 ± 23.7	569.78	57	3.79 ± 0.98
103.94 ± 29.9	910.79	60	4.27 ± 1.24

Table S3. Surface tension components of the three test liquids used for contact angle measurements [14].

Test liquids	Surface tension values (mJ·m^{-2})			
	γ^{LW}	γ^+	γ^-	γ_L
Water	21.8	25.5	25.5	72.8
ethylene glycol	29.0	1.9	47.0	48.0

diiodomethane	50.5	0.0	0.0	50.8

Table S4. The values of contact angle measured for substrates in the presence of water (θ_W), ethylene glycol (θ_{EG}) and diiodomethane (θ_D) and the calculated surface energy components.

Substrate	Contact Angle (°)			Surface energy components (mJ·m^{-2})		
	θ_W	θ_{EG}	θ_D	γ^{LW}	γ^+	γ^-
Au	88.07 ± 2.0	54.30 ± 6.8	34.84 ± 2.7	42.02 ± 1.0	0.01 ± 0.01	2.06 ± 0.8
Bcl-2	52.12 ± 3.8	31.12 ± 3.5	40.02 ± 2.3	39.47 ± 0.7	0.17 ± 0.1	32.27 ± 2.6
BAX/Bcl-2	66.89 ± 3.1	42.49 ± 3.3	40.13 ± 2.8	39.89 ± 1.1	0.18 ± 0.05	14.49 ± 1.7
BSA/Bcl-2	48.51 ± 1.5	32.72 ± 4.8	40.59 ± 2.4	39.10 ± 1.0	0.11 ± 0.03	34.31 ± 4.8

Table S5 The HADDOCK predicted docking score for BAX/Bcl-2 complexes

HADDOCK parameters	BAX/Bcl-2
HADDOCK score	-132.7 ± 5.6
Cluster size	36
RMSD (Å)	0.6 ± 0.4
Van der Waals energy	-54.8 ± 5.8
Electrostatic energy	-524.7 ± 23.8
De-solvation energy	16.8 ± 1.8
Restraints violation energy	102.4 ± 15.8
Buried Surface Area (Å^2)	2369.9 ±71.9
Z-Score	-1.4

Reference

1. G. I. Bell, *SCIENCE*, 1978, **200**, 618-627.
2. E. Evans and K. Ritchie, *Biophysical Journal*, 1997, **72**, 1541-1555.
3. O. K. Dudko, G. Hummer and A. Szabo, *Phys Rev Lett*, 2006, **96**, 108101.
4. O. K. Dudko, G. Hummer and A. Szabo, *PNAS*, 2008, **108**, 15755–15760.
5. R. W. Friddle, A. Noy and J. J. De Yoreo, *Proc Natl Acad Sci U S A*, 2012, **109**, 13573-13578.
6. J. Yang, S. J. L. Petitjean, M. Koehler, Q. Zhang, A. C. Dumitru, W. Chen, S. Derclaye, S. P. Vincent, P. Soumillion and D. Alsteens, *Nat Commun*, 2020, **11**, 4541.
7. S. J. L. Petitjean, W. Chen, M. Koehler, R. Jimmidi, J. Yang, D. Mohammed, B. Juniku, M. L. Stanifer, S. Boulant, S. P. Vincent and D. Alsteens, *Nat Commun*, 2022, **13**, 2564.
8. Y. Wang, J. Wang, S. Huang, C. Liu and Y. Fu, *Int J Biol Macromol*, 2019, **134**, 28-35.
9. Y. Fu, J. Wang, Y. Wang and H. Sun, *Biomolecules*, 2022, **12**.
10. N. Subhi, A. R. D. Verliefde, V. Chen and P. Le-Clech, *Journal of Membrane Science*, 2012, **403-404**, 32-40.
11. H. Barkai, E. Soumya, M. Sadiki, B. Mounyr and K. S. Ibnsouda, *Journal of Adhesion Science and Technology*, 2016, **31**, 726-734.
12. C. J. Van Oss, M. K. Chaudhury and R. J. Good, *Chemical reviews*, 1988, **88**, 927-941.
13. C. Van Oss, *Colloids and Surfaces A: Physicochemical and Engineering Aspects*, 1993, **78**, 1-49.
14. C. Van Oss and R. Giese, *Clays and Clay minerals*, 1995, **43**, 474-477.
15. C. J. van Oss, R. F. Giese, P. M. Bronson, A. Docoslis, P. Edwards and W. T. Ruyechan, *Colloids and Surfaces B: Biointerfaces*, 2003, **30**, 25-36.
16. C. J. van Oss, A. Docoslis and R. F. Giese Jr, *Colloids and Surfaces B: Biointerfaces*, 2001, **22**, 285-300.